http://dx.doi.org/10.5012/bkcs.2012.33.1.60

# Synthesis of Silver Nanoparticles from the Decomposition of Silver(I) [bis(alkylthio)methylene]malonate Complexes

**Euyjin Lee, Longhai Piao,* and Jinkwon Kim***

*Department of Chemistry and GETRC, Kongju National University, Kongju 314-701, Korea*
**E-mail: piaolh@kongju.ac.kr (L. Piao); jkim@kongju.ac.kr (J. Kim)*
*Received September 16, 2011, Accepted October 28, 2011*

Silver(I) [bis(alkylthio)methylene]malonates were synthesized from the reaction of silver nitrate and potassium [bis(alkylthio)methylene]malonates. The structures of the Ag complexes were characterized with nuclear magnetic resonance (NMR), inductively coupled plasma atomic emission spectrometry (ICP-AES) and elemental analysis. Ag nanoparticles (NPs) were obtained from the decomposition of the Ag complexes in 1,2-dichlorobenzene at 110 °C without an additional surfactant. The average sizes of the Ag NPs are in the range of 5.1-6.3 nm and could be controlled by varying the length of the alkyl chain. The optical properties, crystalline structure and surface composition of Ag NPs were characterized with ultraviolet-visible (UV-visible) spectroscopy, transmission electron microscopy (TEM), X-ray diffraction (XRD), gas chromatography-mass spectrometry (GC-MS), X-ray Photoelectron Spectroscopy (XPS) and thermal gravimetric analysis (TGA).

**Key Words :** Silver, Dicarboxylate complexes, Nanoparticles, Thermal decomposition

## Introduction

Nanoscale materials have attracted considerable interest for their potential applications in the fields of electronics, catalysis, pharmaceuticals, *etc*.[1] Most of the applications are based on the quite different chemical and physical properties of the nanomaterials from those of the bulk and atomic species, which stem from their unique electronic structure and extremely large surface area. The properties of nanomaterials strongly depend on their composition, size and shape.[2,3] So, it is of enormous importance and an essential requirement for nanotechnology to produce nanomaterials with desired composition, size and distribution. Up to now, considerable efforts have been made to develop controlled and reproducible synthetic methods for nanomaterials, especially for metal nanoparticles (NPs), like Au NPs and Ag NPs *etc*.[4-6]

Ag NPs are one of the most commonly used nanomaterials in a wide range of consumer products such as medicines, bactericides and electronics.[7-9] Recently, Ag NPs are further utilized in printed electronics owing to their low sintering temperature, high electrical conductivity, and chemical inertness.[10,11] Generally, Ag NPs are prepared from wet chemical reduction of $Ag^+$ using various reduction agents, like $NaBH_4$ and ethylene glycol in an aqueous or polar solvent with the addition of polymers (such as polyvinyl pyrrolidone) as stabilizing agents.[12]

Recently, Nakamoto *et al*. reported the direct synthesis of Ag NPs from the decomposition of a specially designed coordination compound without an additional stabilizing agent.[13-16] The Ag NPs were produced by the reduction of Ag(I) carboxylates with a reducing agent or by pure heat treatment. Their size could be controlled by altering the chain length of the carbxoylate ligands. When the chain length was longer than 14 carbon atoms, monodisperse Ag NPs with diameters of several nanometers could be obtained.

Up to now, Ag NPs have been generally synthesized from molecular precursors such as Ag(I) mono-carboxylate complexes having 0D or 1D structure. However, there are no examples of the usage of molecular precursors using multi-carboxylate ligands. Multi-carboxylate ligands tend to form more inert complexes with transition metal ions than mono-carboxylate ligands.[17] They could coordinate to different metal ions simultaneously with various dimensionality and have the potential to prepare metal alloy NPs. Furthermore, Ag(I) complexes with well designed functional ligands may give enhanced processibility in the silver coating process.

In this paper, we report the synthesis and characterization of novel Ag(I) dicarboxylate complexes and the preparation of Ag NPs by thermal decomposition of the precursors in 1,2-dichlorobenzene solvent.

## Experimental

**Materials and Methods.** KOH (90%), diethyl malonate (99%), 1,4-dioxane (99.0%), carbon disulfide (98%), 1-iodopentane (98%), 1-iododecane (98%), 1-iodotetradecane (98%) and 1,2-dichlorobenzene (99%) were purchased from Sigma-Aldrich. $AgNO_3$ (99.9%), acetone, ethyl alcohol and ethyl ether were obtained from Samchun Chemical Co. (Korea). All of the reagents were used as received. NMR spectra were recorded on a Varian Mercury spectrometer with standard pulse sequence operating at 400 MHz at room temperature with $D_2O$ or $CDCl_3$ as solvents and $H_2O$ or tetramethylsilane as the internal references. The Ag and potassium content of the complexes were analyzed with ICP-AES (Optima 7300 DV, Perkin Elmer, America). Elemental

analyses (C, H, S) were performed on an elemental analyzer (EA, Flash 2000, Thermofisher, Italy). UV-visible absorption spectra were obtained at room temperature using a UV-visible spectrometer (S4100, Scinco, Korea) in the range of 300-900 nm. TEM characterization was performed on a FEI Tecnai $G^2$ F30 S-Twin microscope operated at 300 kV. The average diameter and distribution of the Ag NPs were calculated from at least 100 particles from the TEM image. The crystallinity of the Ag complexes and Ag NPs was analyzed by a powder X-ray diffractometer (Rigaku, DMAX 2000). The amount and composition of the organic surfactant layer were characterized with TGA (Labsys TG-DSC 1600, under nitrogen gas at a heating rate of 10 °C/min), XPS (Multilab ESCA 2000 X-ray photoelectron spectrometer with Mg Kα X-rays as the excitation source) and GC-MS (Agilent 7890A-5975C).

**Synthesis of Ketene Mercaptal Salt (1). 1** was synthesized according to the reported method with modification.[18,19] A solution of diethylmalonate (0.1 mol) and carbon disulfide (0.1 mol) in dioxane (50 mL) was added drop wise to a suspension of KOH (0.2 moL) flakes in dioxane (100 mL) with stirring. The reaction was conducted at 20 °C for 1 h. The yellowish precipitate was filtered, washed with ethyl ether and dried under reduced pressure. $^1$H NMR (400 MHz, $D_2O$, ppm): δ 1.11 (3H, *t*), 3.96 (2H, *q*).

**Synthesis of Ethyl[bis(alkylthio)methylene]malonate (2a-c).** The stoichiometric reaction mixture of 0.04 mol of **1** and 0.08 mol of 1-iodoalkane was stirred in acetone at 0 °C for 24 h. The resulting yellow solution was filtered and dried by rotary evaporation to give a yellow oil. **2a**: Yield, 77%; $^1$H NMR (400 MHz, $CDCl_3$, ppm) δ 0.89 (3H, *t*), 1.32 (7H, *m*), 1.63 (2H, *m*), 2.89 (2H, *t*), 4.26 (2H, *q*), **2b**: Yield, 70%; $^1$H NMR (400 MHz, $CDCl_3$, ppm) δ 0.88 (3H, *t*), 1.32 (17H, *m*), 1.62 (2H, *m*), 2.90 (2H, *t*), 4.27 (2H, *q*), **2c**: Yield, 65%; $^1$H NMR (400 MHz, $CDCl_3$, ppm) δ 0.87 (3H, *t*), 1.32 (25H, *m*), 1.61 (2H, *m*), 2.89 (2H, *t*), 4.26 (2H, *q*).

**Synthesis of Potassium[bis(alkylthio)methylene] malonate (3a-c).** To a solution of 0.02 mol of **2** in ethanol (10 mL) was added 0.05 mol of KOH in ethanol (50 mL) drop-wise. The mixture was stirred at 60 °C for 1 h. The precipitates were washed with diethyl ether and finally dried under reduced pressure. **3a**: Yield, 57%; $^1$H NMR (400 MHz, $D_2O$, ppm) δ 0.74 (3H, *t*), 1.21 (4H, *m*), 1.4 (2H, *m*), 2.66 (2H, *t*) EA (%) Found (Calc.) for $C_{14}H_{22}S_2K_2O_4$: C, 40 (42); H, 5.6 (5.7); S, 11(16), **3b**: Yield, 47%; EA (%) Found (Calc.) for $C_{24}H_{42}S_2K_2O_4$: C, 50 (53); H, 7.7 (7.8); S, 8 (11), **3c**: Yield, 40%; EA (%) Found (Calc.) for $C_{32}H_{58}S_2K_2O_4$: C, 51 (58); H, 7.8 (8.9); S, 5 (9.8).

**Synthesis of Silver[bis(alkylthio)methylene]malonate (4a-c).** A mixture of 0.01 mol of **3** and 0.02 mol of $AgNO_3$ in 1:1 water/ethanol solution (100 mL) was reacted for 24 h. The precipitate was washed with water and dried under reduced pressure. **4a**: Yield, 88%; EA (%) Found (Calc.) for $C_{14}H_{22}S_2O_4Ag_2$: C, 30 (31); H, 4.0 (4.1); S, 11.8 (12.1), **4b**: Yield, 78%; EA (%) Found (Calc.) for $C_{24}H_{42}S_2O_4Ag_2$: C, 42.3 (42.8); H, 5.8 (6.2); S, 8.5 (9.5), **4c**: Yield, 72%; EA (%) Found (Calc.) for $C_{32}H_{58}S_2O_4Ag_2$: C, 46.0 (48.9); H, 7.0 (7.3); S, 6.5 (8.1).

**Preparation of Ag NPs.** A suspension of 500 mg of **4** in 1,2-dichlorobenzene 30 mL was heated at 110 °C with vigorous stirring for 2 h. The resulting NPs were precipitated with ethanol and separated by centrifugation at 3500 rpm for 5 min. The precipitates were washed 3 times with ethanol and finally dried overnight under reduced pressure.

## Results and Discussion

**Synthesis of Ag(I) Dicarboxylate Precursor.** The synthetic route for silver(I) [bis(alkylthio)methylene]malonate (**4**), is presented in Scheme 1. **4** was synthesized by the reaction of silver nitrate and potassium [bis(alkylthio)methylene]malonates (**3**) which was generated by the reaction of diethylmalonate and carbon disulfide in dioxane followed by alkylation with iodoalkane and hydrolysis.

Figure 1 shows the $^1$H NMR spectra of **1**, **2a** and **3a**. In Figure 1(a), the peaks at 3.96 and 1.11 ppm are assigned to the methyl and methylene groups of the ketene mercaptal salt **1**, respectively. **1** readily reacts with pentyliodide to form ethyl[bis(pentylthio)methylene]malonate (**2a**). The $^1$H

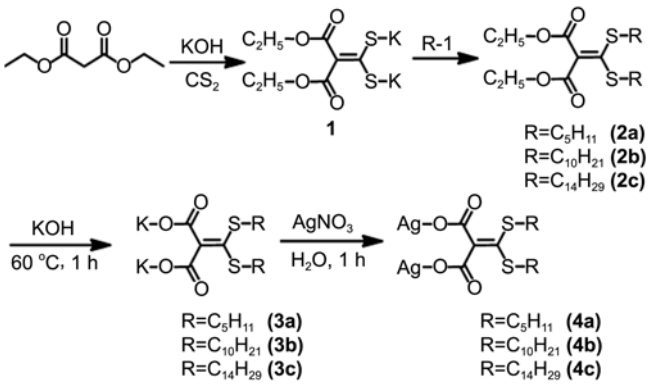


**Scheme 1.** Synthesis of Ag(I) dicarboxylate precursors.

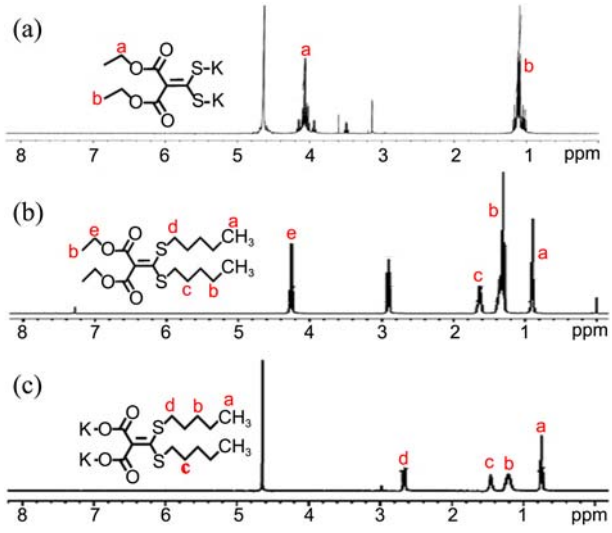


**Figure 1.** $^1$H NMR spectrum of (a) ketene mercaptal salt (**1**), (b) ethyl[bis(pentylthio)methylene]malonate (**2a**), and (c) potassium [bis(pentylthio)methylene]malonate (**3a**).

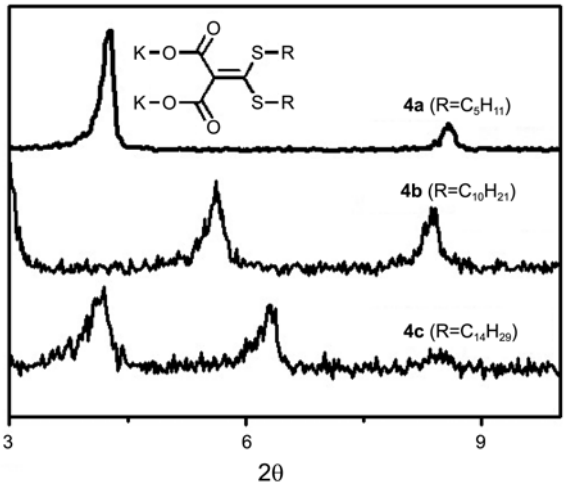


**Figure 2.** XRD pattern of **4a**, **4b** and **4c**.

NMR spectrum of **2a** is shown in Figure 1(b). The triplet peak at 2.89 ppm is due to the methylene protons adjacent to the sulphur atom and the peaks at 1.62 and 1.32 ppm are assigned to the methyl and methylene groups of the alkyl chain, respectively. Figure 1(c) shows the $^1$H NMR spectrum of **3a**; after hydrolysis with KOH, the peaks from the ethyl group of diethylmalonate disappeared. The potassium ion of **3** was exchanged with Ag+ to result in white insoluble precipitates. The elemental analysis data of the Ag(I) dicarboxylate (**4a-c**) are consistent with the calculated results. (see Experimental section) The Ag contents of **4a-c** determined by ICP-AES are also in agreement with the corresponding formulas of the complexes.

The XRD patterns for **4a-c** show regular reflection peaks (Figure 2). Similar to Ag(I) mono-carboxylate, these reflections could be explained in terms of regularly stacked silver dicarboxylate (0*k*0) layers with a large interlayer lattice dimension. The interlayer spacings for **4a-c** calculated from the Bragg equation (eq. 1) were 2.06 nm, 3.16 nm and 4.19 nm respectively. These data are slightly larger than the interlayer spacings for Ag(I) mono-carboxylates with the same alkyl chain length.[20-22]

$$2d\sin\theta = n\lambda \quad (1)$$

where d is the average interlayer spacing, n = *k*, λ is the wavelength of the X-rays (1.5406 Å for CuKα radiation), and θ is the peak position.

**Preparation of Ag Nanoparticles.** Ag NPs were prepared by thermal decomposition of the Ag dicarboxylates of **4a**, **4b** and **4c** in 1,2-dichlorobenzene at 110 °C. The Ag complexes have very low solubility in 1,2-dichlorobenzene and the Ag NPs were produced on the surface of the white slurry of the Ag complex. The solution colour changed gradually from a light yellow to brown. The reaction was stopped when no additional colour change was observed.

It is well-known that noble metal nanoparticles absorb light in the visible region due to localized plasmon resonance dependent upon their size, shape, inter-particle distance and the surrounding dielectric medium. So, the formation of

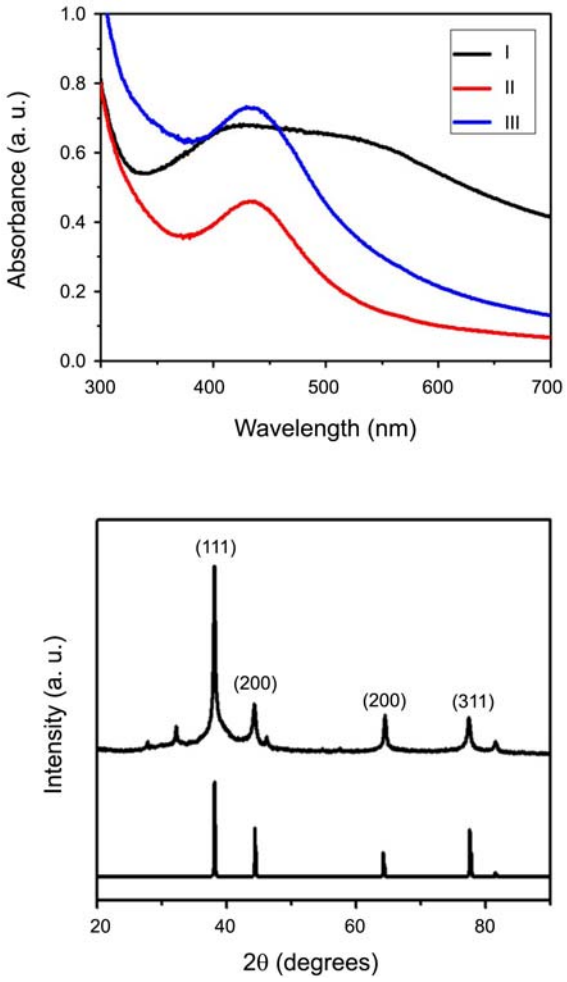


**Figure 3.** (a) UV-vis absorption spectrum of **I**, **II** and **III** dispersed in toluene. (b) XRD patterns of sample **III**. The lower panel represents the standard data for Ag (JCPDS No: 1-1167).

Ag NPs could be easily confirmed by UV-visible spectroscopy. Figure 3(a) shows the UV-visible absorption spectra of Ag NPs decomposed from **4a (I)**, **4b (II)** and **4c (III)**. The characteristic plasmon absorption peaks around 420 nm were observed in sample **II** and **III**, suggesting the formation of Ag NPs. The UV peak for **I** is broad and shifted to longer wavelength. This might be the result of the broad size distribution and the aggregation due to low dispersion stability. The formation of Ag NPs was also confirmed by XRD analysis; the XRD pattern of sample **III** shows the characteristic (111), (200) and (311) planes of face-centered cubic silver (Figure 3(b)).

Figure 4 shows the TEM images of the Ag NPs and a histogram of their diameters. The diameters of the Ag NPs decomposed from **4a**, **4b** and **4c** are 6.3(1.2) nm, 5.7(0.4) nm and 5.1(0.3) nm, respectively. It is clear that the sizes of the Ag NPs decreased with increasing chain length of the dicarboxylate ligand of the precursor. These results are consistent with the previous researches; the systemic studies by Nakamoto *et al*. also showed particle size regulation by changing the chain length of Ag(I) carboxylate ligand.[15] Only spherical Ag NPs with a narrow size distribution were

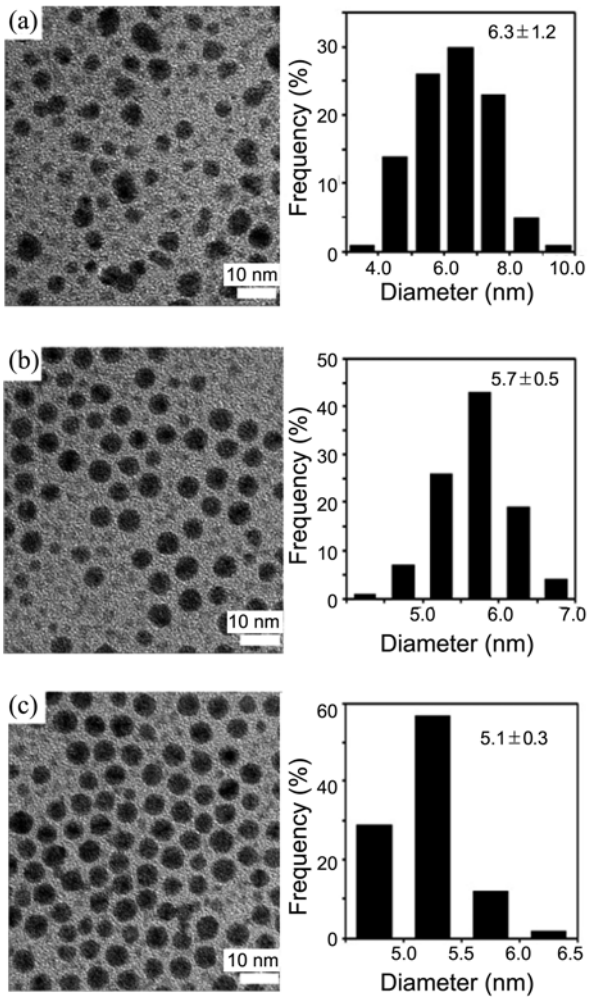


**Figure 4.** TEM images and the size distribution histograms of Ag NPs synthesized from **4a** (a), **4b** (b) and **4c** (c). All the scale bars indicate 10 nm.

observed for the Ag NPs decomposed from **4b** and **4c**. In the case of the dicarboxylate ligand with a short alkyl chain (**4a**), larger and polydisperse Ag NPs were obtained. In the TEM images, multiply twinned structures are clearly shown, implying the Ag NPs are in a multi-crystalline structure (see Supporting Information).

**Surface Analysis of Ag NPs.** The physical and chemical properties of nanostructures strongly depend on their surface and interfacial environment. For that reason, understanding

**Table 1.** Characterization of the Ag complex precursors and Ag NPs

| No. | Precursor | Ag content of the precursor (%)[a] | | Amount of surfactant (%)[b] | Diameter (nm)[c] |
|---|---|---|---|---|---|
| | | Calculated | Found | | |
| sample **I** | **4a** | 40 | 40 | | 6.3 ± 1.2 |
| sample **II** | **4b** | 32 | 34 | 30 | 5.7 ± 0.4 |
| sample **III** | **4c** | 27 | 28 | 35 | 5.1 ± 0.3 |

[a]Determined by ICP-AES. [b]Measured with TGA. [c]Calculated from TEM images.

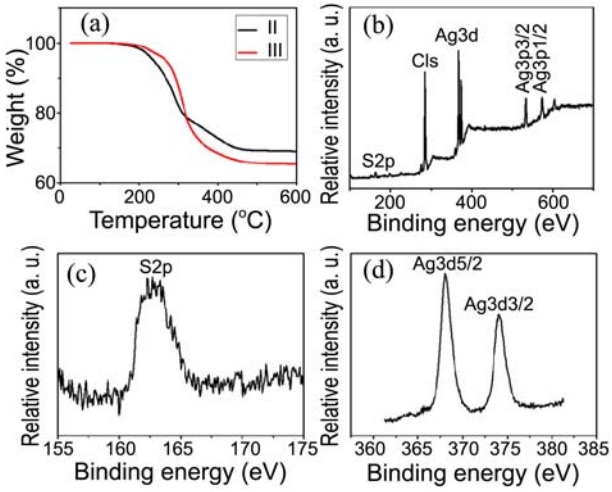


**Figure 5.** (a) TGA curves of samples **II** and **III** (b) XPS survey of sample **III** (c) S 2p (d) Ag 3d spectra.

the organic surfactant layers of nanomaterials is one of the key issues in nanoscience.

The surface composition of the Ag NPs was analyzed by TGA, XPS and GC-MS. Figure 5(a) shows the TGA curves of samples **II** and **III**. Below 300 °C, the organic component was removed completely. Interestingly, the amounts of the organic parts of the Ag NPs obtained in this research are much higher than those of the Ag NPs coated with a mono-carboxylate surfactant with the same carbon chain length. The Ag NPs produced from Ag(I) mono-carboxylate usually show about 20% of the surfactant layers because it is the corresponding carboxylate ligand that attaches to Ag NP surfaces and acts as a surfactant.[23] In order to characterize the surfactant layer composition, GC-MS analysis was conducted. Instead of the corresponding dicarboxylate surfactants, smaller molecular fragments such as thiol or dithiol were detected (see Supporting Information). XPS studies of sample **III** also show the binding energy of S ($2p_{1/2}$) at 162.7 eV, and no peaks corresponding to O binding energies were detected. The binding energies of Ag ($3d_{3/2}$) and Ag ($3d_{5/2}$) are shown at 373.8 eV and 367.8 eV, respectively. Since the reported binding energy of $Ag^0$ ($3d_{5/2}$) is 368.3 eV, the shift in binding energy indicates a bond between Ag and S (Figure 5(b-d)).[24]

From the above GC-MS and XPS analysis, it could be concluded that the dicarboxylate ligand was decomposed during the reaction and that the corresponding thiols adsorb on the Ag NP surface as surfactants. It is interesting to note that the reactions were conducted at 110 °C. Considering the potassium dicarboxylates of **3** were decomposed above 300 °C (see Supporting Information), decomposition of the Ag complex precursor might be catalyzed by Ag atoms. The low temperature decomposition of the Ag complexes might be useful for many applications, such as low sintering temperature Ag paste and ink for printable electronics. Detailed studies of the decomposition mechanism and applications of the Ag complexes are in progress.

## Conclusion

In summary, silver(I) [bis(alkylthio)methylene]malonates were synthesized from the reaction of silver nitrate and potassium [bis(alkylthio)methylene]malonates. From XRD analysis it could be concluded that the Ag complexes synthesized have a regularly stacked layered structure. Ag NPs were obtained from the decomposition of the Ag complexes in 1,2-dichlorobenzene at 110 ºC without an additional surfactant. The average diameters of the Ag NPs are in the range of 5.1-6.3 nm and could be controlled by varying the length of the alkyl chain. According to TGA, XPS and GC-MS analysis, the Ag NP surface was composed of thiol surfactant. This might be caused by the dicarboxyalte ligand decomposition during the reaction.

**Supporting Information Available.** Figure S1, TEM images of the Ag NPs; Figure S2, GC-MS analysis of the Ag NPs; Figure S3, TGA curves of **3a-c**.

**Acknowledgments.** This work was supported by the National Research Foundation (NRF) of Korea funded by the MEST (the Priority Research Centers Program 2009-0093825 and 2010-M2-20100028702).

## References

1. Rosi, N. L.; Mirkin, C. A. *Chem. Rev.* **2005**, *105*, 1547.
2. Puntes, V. F.; Krishnan, K. M.; Alivisatos, A. P. *Science* **2001**, *291*, 2115.
3. Burda, C.; Chen, X. B.; Narayanan, R.; El-Sayed, M. A. *Chem. Rev.* **2005**, *105*, 1025.
4. Zhang, W.; Qiao, X. *J. Chen, Mater. Sci. Eng. B* **2007**, *142*, 1.
5. Bronstein, L. M.; Kostylev, M.; Shtykova, E.; Vlahu, T.; Huang, X.; Stein, B. D.; Bykov, A.; Remmes, N. B.; Baxter, D. V.; Svergun, D. I. *Langmuir* **2008**, *24*, 12618.
6. Briñas, R. P.; Hu, M. H.; Qian, L. P.; Lymar, E. S.; Hainfeld, J. F. *J. Am. Chem. Soc.* **2008**, *130*, 975.
7. Shrivastava, S.; Bera, T.; Singh, S. K.; Singh, G.; Ramachandrarao, P.; Dash, D. *ACS Nano* **2009**, *3*, 1357.
8. Smetana, A. B.; Klabunde, K. J.; Marchin, G. R.; Sorensen, C. M. *Langmuir* **2008**, *24*, 7457.
9. Murray, B. J.; Walter, E. C.; Penner, R. M. *Nano Lett*. **2004**, *4*, 665.
10. Dearden, A. L.; Smith, P. J.; Shin, D. Y.; Reis, N.; Derby, B.; O'Brien, P. *Macromol. Rapid Commun.* **2005**, *26*, 315.
11. Kamyshny, A.; Ben-Moshe, M.; Aviezer, S.; Magdassi, S. *Macromol. Rapid Commun.* **2005** , *26*, 281.
12. Rycenga, M.; Cobley, C. M.; Jie, Z.; Weiyang, L.; Christine, H. M.; Qiang, Z.; Dong, Q.; Xia, Y. N. *Chem. Rev.* **2011**, *111*, 3669.
13. Yamamoto, M.; Nakamoto, M. *J. Mater. Chem.* **2003**, *13*, 2064.
14. Kashiwagi, Y.; Yamamoto, M.; Nakamoto, M. *J. Colloid Interface Sci.* **2006**, *300*, 169.
15. Yamamoto, M.; Kashiwagi, Y.; Nakamoto, M. *Langmuir* **2006**, *22*, 8581.
16. Abe, K.; Hanada, T.; Yoshida, Y.; Tanigaki, N.; Takiguchi, H.; Nagasawa, H.; Nakamoto, M.; Yamaguchi, T.; Yase, K. *Thin Solid Films* **1998**, *327-329*, 524.
17. Jensen, K. A.; Henriksen, L. *Acta Chem. Scand*. **1968**, *22*, 1107.
18. Soderback, E. *Acta Chem. Scand*. **1962**, *17*, 362.
19. Gompper , R.; Topfl, W. *Chem. Ber*. **1962**, *95*, 2861.
20. Lee, S. J.; Han, S. W.; Choi, H. J.; Kim, K. *J. Phys. Chem. B*. **2002**, *106*, 2829.
21. Lee, S. J.; Han, S. W.; Choi, H. J.; Kim, K. *J. Phys. Chem. B*. **2002**, *106*, 7439.
22. Kim, J.; Park, C.-H.; Kim, S.-H.; Yoon, S.; Piao, L. *Bull. Korean Chem. Soc.* **2011**, *32*, 3267.
23. Piao, L.; Lee, K. H.; Min, B. K.; Kim, W.; Do, Y. R.; Yoon, S. *Bull. Korean Chem. Soc.* **2011**, *32*, 117.
24. He, S.; Yao, J.; Xie, S.; Gao ,H.; Pang, S. *J. Phys. D*. **2001**, *34*, 342.